MODELLING MECHANICAL STRESSES DUE TO INTERCALATION AND DE-INTERCALATION OF LITHIUM-IONS IN A CARBON FIBER BATTERY

A. Pupurs[1*], J. Varna[1]

[1]*Department of Engineering Sciences and Mathematics, Division of Materials Science, Luleå University of Technology, SE 97187, Luleå, Sweden*
**e-mail andrejs.pupurs@ltu.se*

Keywords: carbon fiber, ion intercalation, mechanical stress, fracture mechanics.

Abstract
Gradients in Li+ ion concentration distribution in a carbon fiber are accompanied by non-uniform fiber swelling leading to development of mechanical stresses. During lithium deintercalation these stresses may lead to initiation and growth of radial cracks in the fiber. This phenomenon decreases the mechanical properties of fibers if used in structural batteries and reduces the charging properties of the battery by initiating exfoliation of layers on the fiber surface. The radial crack propagation and possible damage evolution scenarios are analyzed using linear elastic fracture mechanics.

1 Introduction

One of the materials with a potential for use as electrodes in Li-ion batteries is carbon fiber. In future structural batteries these carbon fibers will have also a load bearing function. Fiber degradation in addition to reduced load bearing function may affect also the ion diffusivity and the number of charge-discharge cycles with high energy efficiency. During the intercalation process Li+ ions enter the fiber via interface by diffusion process, see Fig. 1a. In the beginning the ion concentration has a gradient with high concentration at the fiber surface. Ion concentration gradient in the material leads to anisotropic volumetric changes (swelling) in the transversally isotropic carbon fiber characterized by β_3 and β_1 in axial and radial directions respectively. Due to the concentration gradient the outer region of the fiber has larger free swelling strains than the inner region. Since displacement continuity has to be satisfied radial stresses σ_r are positive (the outer region by tempting to expand more applies radial tractions to the inner part) whereas hoop stresses σ_θ are negative in the outer region and positive in the inner region. At the end of the diffusion process the concentration gradient decays and so do all mechanical stresses. The radial diffusion process and corresponding stress distributions in the fiber as well as in spherical particles have been analyzed previously, for example in [1,2] using series expansion obtaining concentration distribution as a function of the radial coordinate.

During the deintercalation, Fig. 1b (1/4 of fiber cross-section is shown), the outer region loses ions first and would shrink which is constrained by the inner region which is still in the swelled state. Equilibrium is reached with outer regions being under tensile hoop stresses (compressive σ_θ in the inner regions). Strength based failure criteria are applicable to analyze possible sites, time instants and mechanisms of failure initiation. The damage development

has to be approached by fracture mechanics methods. In repeated charging and discharging cycles we may expect radial crack initiation and growth during discharging (deintercalation). The crack growth can start in quasi-static manner from the surface or in a fatigue manner during deintercalation in repeating cycles.
The diffusion process can be very complex, generally speaking, the system to analyze contains an electrolyte where the ion concentration can change and have a gradient and the fiber/electrolyte system may be surrounded by other solid materials with certain mechanical properties and their own ion diffusion parameters.

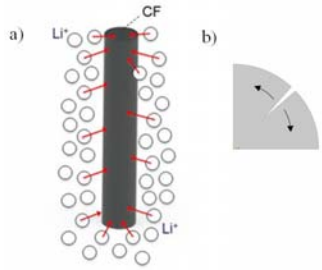

Figure 1. Li+ ion diffusion: a) schematic geometry; b) crack due to positive hoop stresses during deintercalation.

The objective of the presented paper is to analyze the Li+ ion diffusion in the carbon fiber solving numerically the time and coordinate dependent diffusion problem. The static elasticity problem is solved in selected instants of time corresponding to certain concentration distribution, the stresses are analyzed. Radial cracks are introduced and trends in their growth are analyzed using Virtual Crack Closure Technique (VCTT) well known in Fracture Mechanics.
In this paper we simplify the problem by considering a single fiber in an infinite source of ions. The focus is on internal stresses in the fiber due to concentration gradients and not to the mechanical constraint of surrounding materials which are parts of the structure of the battery. We assume a very low transfer resistance of the electrolyte. Hence, the ion concentration in the electrolyte does not change during intercalation or de-intercalation.

2 Theoretical background

2.1 Ion concentration in the carbon fiber

We consider an infinite electrolyte with uniformly distributed carbon fibers characterized by fiber content V_f. This system can be represented by a cylindrical unit cell with a long fiber surrounded by an electrolyte which may have also nonzero elastic and swelling constants. During the intercalation Li+ ions move into the fiber and their distribution along the radial coordinate can be described by concentration distribution which follows diffusion equation

$$\partial C/\partial t = D\Delta C \tag{1}$$

In (1) C is the relative ion concentration in the fiber with respect to available sites, Δ is Laplace operator and D is diffusion coefficient.
If the fiber is undamaged or if cracks are in radial direction the diffusion is in radial direction only and the concentration does not depend on θ. Eq.(1) is a particular case of a more general equation [3].
At the fiber surface $r=r_f$ we require that the Li+ flux N is related to the local current density in the electrolyte

$$N = i/F \tag{2}$$

The flux at the fiber surface according to [3] is

$$N = -Dc_0 \nabla C \tag{3}$$

In (3) ∇ is the gradient operator, c_0 is the total site concentration in the host material (the maximum concentration of lithium ions inside the fiber if all sites would be occupied). Using for the current flow expression from [1] we obtain boundary condition

$$Dc_0 \nabla C + (k_a^{'} + k_c^{'})(C - C_R) = 0 \text{ at } r = r_f \tag{4}$$

Constants in (4) are introduced in [1]. Parameter C_R has a meaning of saturation concentration of ions in the fiber.
Introducing normalized coordinate and time

$$x = r/r_f \quad \tau = tD/r_f^2 \tag{5}$$

the diffusion (1) and the boundary condition (4) can be written in dimensionless form

$$\partial C/\partial \tau = \Delta_x C \tag{6}$$

$$\nabla_x C + B(C - C_R) = 0 \text{ at } r = r_f \quad B = (k_c^{'} + k_a^{'}) r_f / Dc_0 \tag{7}$$

Operators with index x are defined replacing r by the normalized radial coordinate x.
By this procedure all unknown parameters listed above are reduced to one unknown parameter B (Biot constant). Varying this parameter from zero to infinity we can cover all possible combinations of parameters, k_c', k_a', D, c_0 and r_f.
As an initial condition for intercalation we assume that at t=0 the concentration is zero

$$C(r, t = 0) = 0 \tag{8}$$

Since the diffusion problem is linear, we can assume C_R=1 when calculating the concentration distribution during intercalation.
During deintercalation the electrochemical parameters change affecting the C_R and B values. As an extreme case we assume in calculations C_R=0 and vary Biot constant B. The initial condition in this case is

$$C(r, t = 0) = 1 \tag{9}$$

2.2 Stress distribution in the carbon fiber
Plane strain solution is obtained if ε_{z0}=0, generalized plane strain solution corresponds to the case when ε_z=const obtained from requirement that the axial force is equal to zero.
Stress-strain relationships for transversally isotropic fiber (index 1, 2 and 3 correspond to r, θ and z directions) are

$$\varepsilon_r - \beta_1 c_0 C = -\frac{\nu_{31}}{E_3}\sigma_z + \frac{1}{E_1}\sigma_r - \frac{\nu_{12}}{E_1}\sigma_\theta \tag{10}$$

$$\varepsilon_\theta - \beta_1 c_0 C = -\frac{\nu_{31}}{E_3}\sigma_z + \frac{1}{E_1}\sigma_\theta - \frac{\nu_{12}}{E_1}\sigma_r \tag{11}$$

$$\varepsilon_z - \beta_3 c_0 C = -\frac{1}{E_3}\sigma_z + \frac{\nu_{31}}{E_1}\sigma_r - \frac{\nu_{31}}{E_1}\sigma_\theta \tag{12}$$

In (10)-(12) β_i, i=1,3 are free swelling coefficients of the fiber.
The diffusion problem and the elastic problem are decoupled. We can first find the concentration distribution using (6), (7). The concentration distribution $C(r,\theta,\tau)$ is used as input in the elastic problem which can be solved at any arbitrary instant of t. If the electrolyte elastic modulus is very low it should not constrain the deformation of the fiber.

2.3 Thermo-mechanical analogy
Solving the intercalation problem we can select C_R=1 and the ion concentration in the fiber will vary between 0 and 1. The concentration profiles for other values of C_R are proportional to the calculated and can be obtained by simple multiplication.
Similar conclusions apply to the elastic stress problem: elastic stresses for cases when $C_R \neq 1$ can be obtained by multiplying the obtained stress state by C_R. In parametric analysis we do not need to consider separately parameter C_R and parameters β_i. In the stress expressions the ion concentration C is always multiplied by swelling coefficients β_i, i=r,θ,z and by c_0.
The mathematical description of the concentration distribution (6), (7) is the same as for heat conduction problem with convection boundary conditions: parameter B has the meaning of the heat transfer coefficient, C is analogous to the temperature distribution and C_R is the value of temperature in the surrounding medium, see [4]. This analogy was used to employ finite element code ANSYS to find concentration and stress distributions.

2.4 Fracture mechanics approach
To follow the growth of a certain damage entity (crack) we have to introduce it in the model. After that energy based criteria can be used to analyze the growth quantitatively.
In Fig. 2a a part of the fiber with a radial crack of length l_r is shown ($l_r \in [0,1]$). During the deintercalation the crack is open due to positive hoop stresses and its further growth in the radial direction by dl_θ has to be studied. The propagation is in pure Mode I (opening mode) and it is governed by Mode I energy release rate $G_I(x)$. In quasi-static case the used fracture mechanics criterion is

$$G = G_c \tag{13}$$

In (13) G is the strain energy release rate and G_c is its critical value. It has to be noted that: a) G_c may be mode mixity dependent; b) due to anisotropic fiber it may be direction dependent. In fatigue loading one can assume that the crack growth is governed by a power law

$$dl/dN = A(\Delta G)^m \tag{14}$$

In (14) A, m are material constants, $\Delta G = G_{max} - G_{min}$ is the change of the strain energy release rate between state where it is the highest and the state where it has minimum. The strain

energy release rate contains two components G_I and G_{II} corresponding to the opening and sliding modes respectively

$$G = G_I + G_{II} \tag{15}$$

Each of these components can be calculated using the VCCT: the energy required to create a unit of a new crack surface, dl is equal to the work to close this surface. In the VCCT we assume that the displacement distribution at the tip of the crack which is infinitesimally longer is the same as for the initial crack size.

3 FEM model

A two phase (fiber and matrix electrolyte) model was created using FEM software code ANSYS version 13.0. Since we account for the radial cracks in the fiber the axial symmetry of the problem is lost. First the transient ion concentration problem was solved by generating the carbon fiber phase only and applying the convection boundary condition (7) directly on the outer fiber surface. In other words, solving the diffusion problem the effect of the electrolyte is presented by boundary condition (7). According to Section 2, the results depend only on one parameter, B. We assume that the electro-chemical constants remain unchanged, and hence the different values of B are caused by different values of diffusivity D. As a consequence, the time scales, see (5), are different. This becomes important if we compare results for several cases at distinct time instances. According to Eq.(5) the relation between normalized times for cases with D_1 and D_2 is $\tau_1=(D_2/D_1)\tau_2$. This relationship was used to recalculate all results to the same normalized time. Two cases were analyzed: 1) with B=500; 2) with B=5. The relation between diffusion coefficients for Cases 1 and 2 is $D_1=0.01D_2$. The initial conditions on all nodes of the fiber were specified by (8) or (9) for intercalation and deintercalation respectively.

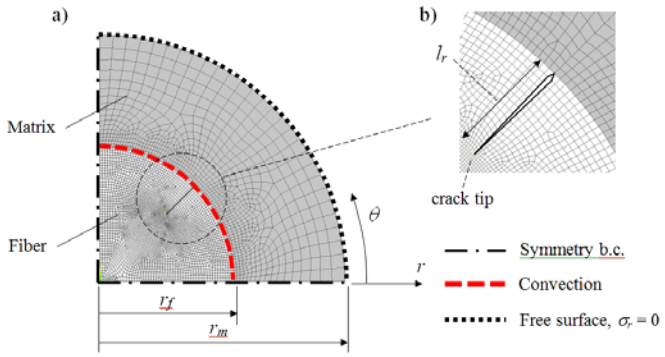

Figure 2. a) FEM model for calculating radial crack growth related energy release rate b) schematic representation of a radial crack.

In the second step the mechanical problem was solved. The matrix phase was added to the fiber phase and the elastic properties of both phases were defined. Stress distributions were found corresponding to selected instants of time with given concentration distribution. Only ¼ of the total transverse FEM model was used in calculations.

Fig.2 shows the geometry of the FEM model, the crack face position corresponds to the angular coordinate of $\theta=\pi/4$. Due to the symmetry conditions on the horizontal and on the vertical axis, the fiber in this model has four cracks with 90° between them.

4 Results and discussion

4.1 Input parameters

The elastic and swelling parameters are listed in Table 1. Subscript f in Table 1 denotes fiber. The stress distributions were also calculated for a case with matrix elastic modulus E_m= 100 MPa.

The axial free swelling strain in Table 1 was obtained by extrapolating the data from [5].

In [5] the swelling strain $\beta_3^f c_0 C_R$ was experimentally estimated as 0.003 for the measured capacity of 135mAh/g at 1 hour charge.

E_3^f **[GPa]**	E_1^f **[GPa]**	G_{31}^f **[GPa]**	ν_{31}^f	ν_{12}^f	$\beta_3^f c_0 C_R$	$\beta_1^f c_0 C_R$	E_m **[GPa]**	ν_m
300	30	20	0.2	0.45	0.009	0.1	1	0.3

Table 1. Elastic properties of constituents for the reference case calculation.

In [6] it was shown that for PAN based IMS65 carbon fiber electrodes the capacity can be increased by up to 3 times when charging slower, meaning that more Li+ ions can be intercalated leading to higher swelling. Based on these findings, the longitudinal swelling strain was assumed equal to $\beta_3^f c_0 C_R$ = 0.009 to account for the most extreme possibility.

4.2 Stress distributions

In Figs.3 and Fig.4 ion concentration, radial stress σ_r and tangential stress σ_θ are presented for intercalation with B=500 and B=5 respectively. The results are reduced to the same time scale: the various instants of the normalized time are calculated as $t^*=\tau_1=0.01\tau_2$. At fixed time instants the concentration distribution in Fig.3 has higher gradients than in Fig.4 because the diffusion coefficient is 100 times higher and the diffusion is much faster. The higher gradients in concentration result in higher values of the stress components in Fig.3 compared to Fig.4. During the intercalation the radial stress is positive with the maximum on the fiber axis. In the central region the hoop stress σ_θ values are similar to the radial stress values. In the interface region they are almost two times higher but they are compressive. Hence, the only damage made that could be expected to initiate in the intercalation phase is cracks in the central region because of combined action of radial and hoop stresses. The values of these stresses are not relatively high and the probability of this damage mode as compared with other possibilities described below is low.

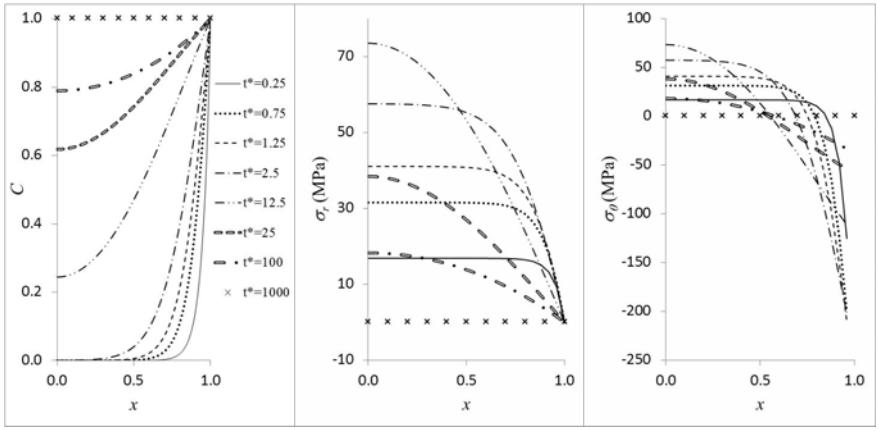

Figure 3. Concentration and stress distributions during intercalation with B = 500.

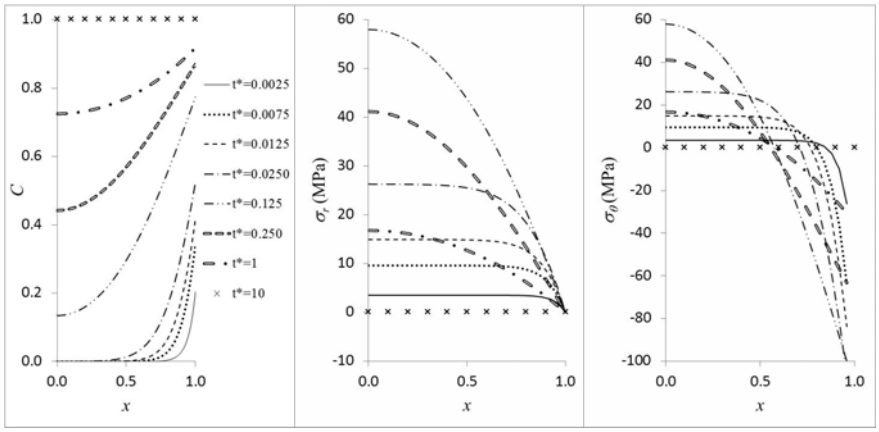

Figure 4. Concentration and stress distributions during intercalation with B = 5.

Results presented in Fig. 3 and 4 are for intercalation. During deintercalation the initial concentration distribution is uniform (C=1); ions start to leave the interface region. The concentration distribution dependence on time can be obtained from data in Fig. 3 and Fig. 4 by creating a mirror picture with respect to the axis C=1 and shifting the result by one unit down. The stress distributions in Fig. 3 and Fig.4 are just changing sign. Hence, the high hoop stresses σ_θ become positive and since they are roughly two times higher than the tensile radial stress during intercalation, we can expect that during deintercalation radial crack can be created in Mode I (due to the assumed symmetry). The effect of the electrolyte elastic properties on the stress distributions was investigated changing the elastic modulus of the electrolyte to 100MPa, see Table 2. Since the influence on the stress distribution is very small, the described sequence of events is not changing. In following calculations the value E_m=1MPa is used.

V_f	E_m **[GPa]**	t^*	$\sigma_r(x=0)$ **[MPa]**	$\sigma_r(x=1)$ **[MPa]**	$\sigma_\theta(x=1)$ **[MPa]**
0.3	1	25	38.47	0.00286	-54.11
0.3	100	25	38.00	0.1262	-54.58

Table 2. Parametric analysis of dependency of stresses on matrix elastic modulus E_m.

4.3 Radial crack growth during deintercalation

The conditions for the radial crack growth were analyzed using the model described in Section 3. Results are presented for B=500 only. Fig.5 shows Mode I energy release rate G for the radial crack growth during deintercalation. According to Fig.5a in the beginning of the deintercalation the G_I curves are monotonously decreasing with the radial crack length l_r. One can visualize the presented curves as evolution of one curve which is changing its values and shape with the time. In the beginning ($t^* \leq 2.5$) this curve has growing values in increasing time instants, after that the values at the same l_r are decreasing. In a quasi-static case (criterion (13)) with G_C the description of events is as follows. Assuming a certain initial crack length l_r^0, see Fig.5a, this crack will start to grow at the time instant when the G_I curve corresponding to the reached concentration distribution crosses the horizontal G_c curve in the point $l_r=l_r^0$. Since in this part of the deintercalation the G_I curve is growing with the time the cross-point with G_c curve is moving with the time to the right, which means that the radial crack is growing. After reaching $t^* \leq 2.5$ the G_I curve starts to decrease, which means that the cross-point is moving to the left. This means that the G_I value for the reached cracks length is lower

than G_C and the crack growth stops. It will not grow further in the following intercalation-deintercalation cycles. If the G_C value is very high, the G_I curve will never cross the G_C curve and the radial defect will never grow in a quasi-static manner. In such case the radial crack can grow during the cycles of charging as the result of fatigue which may be governed by (14). The ΔG during one cycle depends on the crack length. According to (14) the ΔG value determines the rate of the crack growth. For short radial crack it is large and the crack growth rate with the number of deintercalation cycles is high. With increasing radial crack length the ΔG reduces and the growth rate slows down and eventually stops (the values at l_r=0.7 are close to zero).

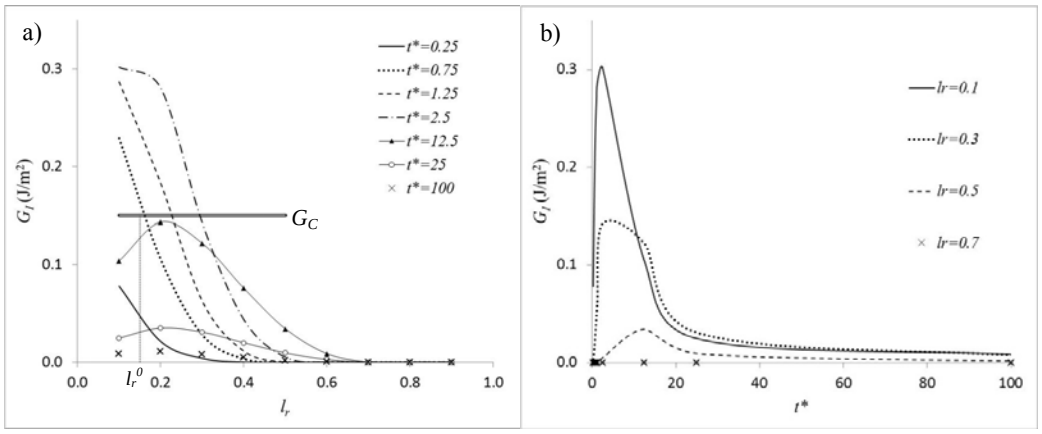

Figure 5. G_I in J/m^2 for radial crack growth during deintercalation, B =500.

5 Conclusions

Analysis of ion concentration distributions and stress distributions showed that radial cracks may appear in the fiber during the deintercalation. Growth of this type of cracks was analyzed calculating strain energy release rate using Virtual Crack Closure technique. In a quasi-static case these cracks are growing stably with time. The growth stops when due to ion concentration gradient change with time the strain energy release rate starts to decrease.

The radial crack can grow also in fatigue with increasing number of intercalation-deintercalation cycles. The fatigue crack growth rate is highest when the crack is short and becomes equal to zero when the radial crack length reaches 70% of the fiber radius.

References

[1] Cheng Y.-T., Verbrugge M.W. *J. Electrochem. Soc.*, **157(4)**, pp. 508-516 (2010).
[2] Christensen J., Newman J., *J. Electrochem. Soc.*, **153(6)**, pp. 1019-1030 (2006).
[3] Verbrugge M.W., Koch B.J. *J. Electrochem. Soc.*, **143(2)**, pp. 600-608 (1996).
[4] Crank J. *The mathematics of diffusion*. Clarendon, Oxford, England (1956).
[5] Jacques E., Kjell M.H., Zenkert D., Lindbergh G., Behm M. in "Proceedings of *The 15th European Conference on Composite Materials (ECCM 15)"*, Venice, Italy, (2012).
[6] Kjell M.H, Jacques E., Zenkert D., Behm M., Lindbergh G. *J. Electrochem. Soc.*, **158(12)**, pp. 1455-1460 (2011)